TU Delft

Delft University of Technology

The role of matrix boundary in the microstructure of unidirectional composites

Gomarasca, S.; Peeters, D.M.J.; Atli-Veltin, B.; Dransfeld, C.A.; Luinge, Hans

Publication date
2022

Document Version
Final published version

Published in
Proceedings of the 20th European Conference on Composite Materials: Composites Meet Sustainability

Citation (APA)
Gomarasca, S., Peeters, D. M. J., Atli-Veltin, B., Dransfeld, C. A., & Luinge, H. (2022). The role of matrix boundary in the microstructure of unidirectional composites. In A. P. Vassilopoulos , & V. Michaud (Eds.), *Proceedings of the 20th European Conference on Composite Materials: Composites Meet Sustainability: Vol 3 – Characterization* (pp. 636-643). EPFL Lausanne, Composite Construction Laboratory.

Important note
To cite this publication, please use the final published version (if applicable).
Please check the document version above.

Copyright
Other than for strictly personal use, it is not permitted to download, forward or distribute the text or part of it, without the consent of the author(s) and/or copyright holder(s), unless the work is under an open content license such as Creative Commons.

Takedown policy
Please contact us and provide details if you believe this document breaches copyrights.
We will remove access to the work immediately and investigate your claim.

This work is downloaded from Delft University of Technology.
For technical reasons the number of authors shown on this cover page is limited to a maximum of 10.

THE ROLE OF MATRIX BOUNDARY IN THE MICROSTRUCTURE OF UNIDIRECTIONAL COMPOSITES

Silvia Gomarasca[a], Daniël Peeters[a], Bilim Atli-Veltin[a,b], Joris Markenstein[c], Hans Luinge[c], Clemens Dransfeld[a]

a: Delft University of Technology, Department of Aerospace Structures and Materials, Delft, Netherlands – s.gomarasca@tudelft.nl
b: Nederlandse Organisatie voor Toegepast Natuurwetenschappelijk Onderzoek (TNO), Delft, Netherlands
c: Toray Advanced Composites, Nijverdal, Netherlands

Abstract: *Finding new ways to evaluate the microstructural characteristics and their effect on macroscopic properties such as permeability and mechanical performance is of increasing interest for fibre reinforced polymer composites. The three-dimensional variability of microstructural features is not fully understood and its effect on macroscale properties is not well established, and so far mostly analysed at a phenomenological level. In order to achieve a more complete definition of the unidirectional composites domain, an understanding of matrix-based features and their interrelation with fibre architecture descriptors is needed. We introduced in recent work a method based on X-ray Computed Tomography for the quantification of fibre-architecture descriptors at an increasing level of complexity. To expand the methodology, this work accounts for matrix-based phenomena such as tape boundary variability and distribution of voids.*

Keywords: Microstructure; Unidirectional Composites; X-ray Computed Tomography; Matrix boundary; Voids.

1. Introduction

Finding new ways to evaluate the microstructural characteristics and their effect on macroscopic properties such as permeability and mechanical performance [1,2] is of increasing interest for fibre reinforced polymer composites. 3D imaging techniques have been receiving increasing interest in evaluating fibre architectures, void distribution and damage formation [3–5]. However, the variability of microstructural features at a three-dimensional level is not fully understood. Its effect on macroscale properties is not well established, and mostly analysed at a phenomenological level [6].

We introduced in recent work a method based on X-ray Computed Tomography for the three-dimensional description of the fibrous microstructure of unidirectional tapes at a single fibre level [7]. Three metrics are introduced in the work to describe the increasing level of complexity in the microstructural organization, from a single fibre path level with differential tortuosity, over group behaviour with collective motion, to fibre network connectivity with the length of neighbourhood. These descriptors and their interdependence highlight local effects like edge-core segregation in microstructural characteristics.

However, to achieve a complete definition of the unidirectional tape domain, capturing matrix-based features such as tape boundary and void distribution is crucial to characterize its properties [8,9]. In particular, recent studies relate the effects of surface resin-rich layers in

 ©2022 1st Author et al. https://doi.org/ 10.5075/978-X-XXX-XXXXX-X published under CC BY-NC 4.0 license

unidirectional tapes to their processability [10,11]. The interrelation between matrix and fibre descriptors will also help generate further insight into microstructure formation, properties and quality assessment.

In this work, we expand the methodology we have recently developed [7] by inter-relating fibre and matrix descriptors: fibre differential tortuosity, to matrix-based characteristics such as tape boundary variability, and void distribution and morphology. The approach is showcased on a unidirectional composite tape.

2. Methodology

To define a data processing method to characterise matrix-based features such as tape surface variability, void distribution and void morphology at a 3D level, the local tape boundary and internal void locations were extracted via image analysis methods. The workflow is showcased with the study of a unidirectional fibre-reinforced tape analysed via X-ray micro-computed tomography. The composite tape studied is an experimental thermoplastic tape reinforced with unidirectional standard modulus carbon fibres manufactured by Toray Advanced Composites.

2.1 X-ray computed tomography

A X-ray micro computed tomography scan was conducted with a Zeiss Xradia 520 Versa machine, at a voxel size of 0.7788 µm, with a resulting tape cross-section width of 1200 µm. A representative cross-section is shown in Figure 1a. The volume was acquired with a voltage of 70 kV, power of 5 W, and exposure time of 7 s. Of the acquired volume, a length of 800 µm in the fibre direction was considered for the analysis.

2.2 Segmentation of the microstructural features

The scan volume was processed via Fiji plugins to extract the features of interest [12]. The focus was to highlight matrix-based features such as tape contour and voids distribution, and fibre positions through the volume. Prior to feature extraction, volume tilt was corrected via re-slicing and manual alignment with the main fibre direction. A data reduction scheme was then applied where one slice every five in the tape length direction was used, resulting in a ‘stretched’ voxel having dimensions of 0.78 µm by 0.78 µm in the plane perpendicular to the principal fibre direction and 3.9 µm in the primary fibre alignment (longitudinal) direction.

The workflow for the extraction of matrix features is described in Figure 1. Fibres were segmented via Trainable Weka segmentation [13] with a result as in Figure 1b. Tape surface and air were segmented in a second step via the same method, resulting in the map of Figure 1c. Thresholding followed by morphological filtering (opening and closing with a spherical structuring element of 2 pxl in diameter) were then applied to reduce the noise in the segmented volume. Area filtering was conducted on the connected components of the tape to remove segmentation artefacts outside the tape region, resulting in a binary output, shown in Figure 1c. The contour of the remaining connected components was then evaluated (Figure 1d) and merged to identify the local boundary of the tape at each cross-section, as in Figure 1e. The local boundary was then used as a mask to isolate the internal voids from the surrounding air, as shown in Figure 1f.

 ©2022 1st Author et al. https://doi.org/ 10.5075/978-X-XXX-XXXXX-X published under CC BY-NC 4.0 license

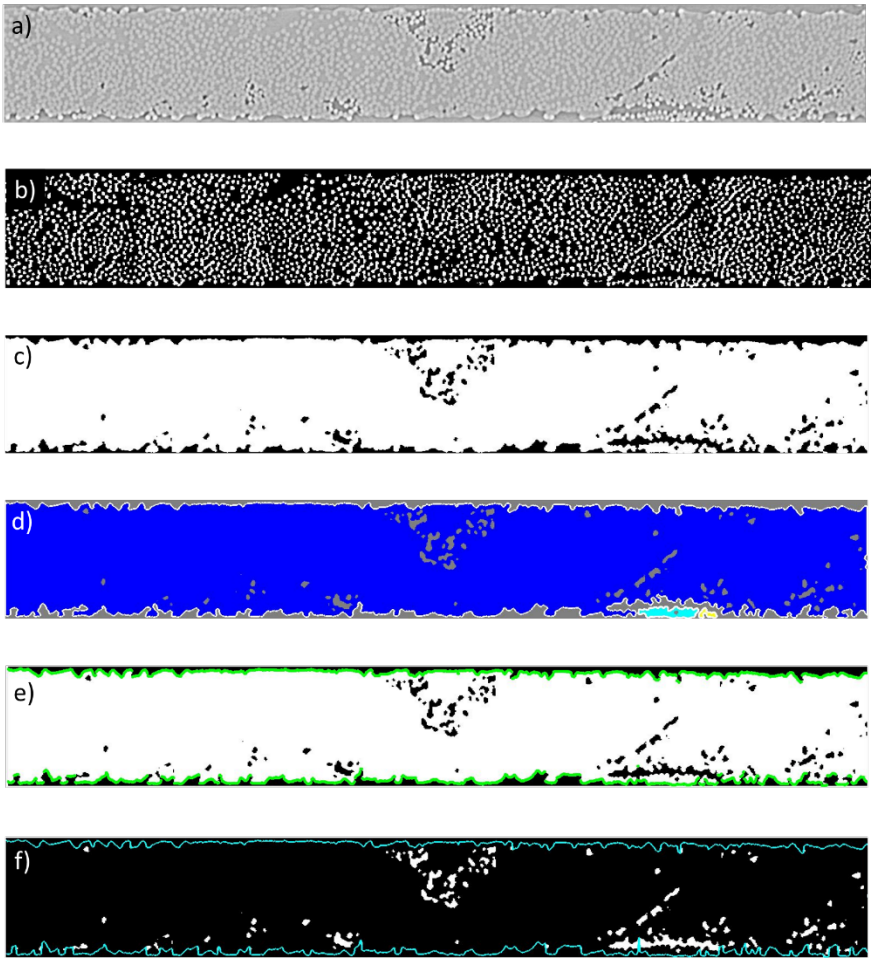

Figure 1. Workflow for tape analysis a) tape cross-section b) segmented fibres, highlighted in white c) tape matrix and fibres (white) and air (black) as obtained after segmentation, thresholding, morphological operations and area filtering d) boundary detection for each connected component, consisting in this case of three regions, labelled respectively in blue, cyan and yellow e) resulting tape boundary of the cross-section, highlighted in green f) internal voids highlighted in white, within the tape boundary in cyan.

2.3 Determination of the microstructural descriptors

2.3.1 Fibres

Fibre paths reconstruction and analysis were conducted as a variation of the methodology described in previous work [7]. Individual fibre path reconstruction was performed by TrackMate [14]**.** A smoothing length of five times the fibre diameter was used to post-process the fibre tracks before the calculation of the parameters. Differential tortuosity was used as a microstructural descriptor of the unidirectional fibre architecture, as defined in our previous work [7]. The parameter is calculated for each fibre:

$$\tau^d = \frac{L - L_o}{L_o} \quad (1)$$

where L is the total detected length of the fibre, and L_o is the perpendicular distance between the two outer sections analysed.

 ©2022 1st Author et al. https://doi.org/ 10.5075/978-X-XXX-XXXXX-X published under CC BY-NC 4.0 license

The parameter quantifies the cumulative local misalignment of fibre paths and can provide a first indication of the local disorder in the fibre arrangement. The tortuosity values were then interpolated at the voxel locations to obtain a 2D homogenised distribution.

2.3.2 Tape boundary

The tape surface variability was determined as local elevation compared to the mean coordinate of the upper and lower boundaries. The range of elevation was then determined for each pixel along the tape width as the difference between the maximum and minimum values. A smoothing length equal to two fibre diameters (15 µm) was used to reduce the noise of the range profile. The surface elevation range was related to the mean logarithm of differential tortuosity at the same voxel locations.

2.3.3 Voids

Voids with the size of a unit voxel were filtered out as noise, while the remaining voids were further analysed in terms of their size, aspect ratio and spatial distribution. The 2D histogram of the distribution of voids over the cross-section was used to map the local void accumulation, defined as the product of the histogram bin-count for each cross-sectional location and the voxel size along the primary fibre alignment direction. The void accumulation was then related to the logarithm of differential tortuosity.

3. Results and discussion

In this section, the results of the analysis of fibre differential tortuosity, and of tape boundary variability and voids are provided and discussed.

3.1 Differential tortuosity

The map of the logarithm of differential tortuosity is reported in Figure 2. The values reported are a homogenization of the values determined in the length of observation considered of 800 µm. The parameter varies along the cross-section. Corridors generated by high tortuosity fibres are highlighted in Figure 2 with dashed yellow lines and are observed along the bottom tape surface, running from the bottom to the top side of the cross-section. Darker regions of lower tortuosity, where fibres are more aligned, are present in-between higher tortuosity regions.

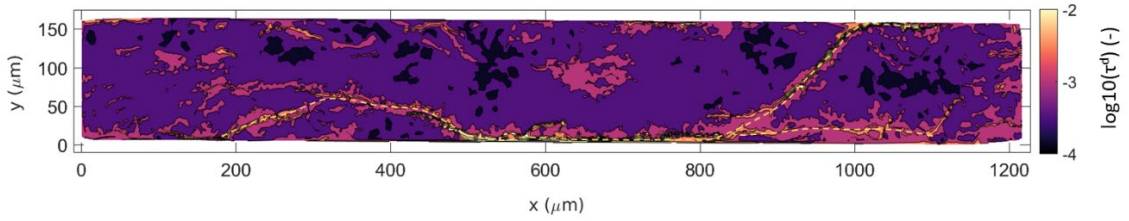

Figure 2. Map of the logarithm of differential tortuosity. High tortuosity corridors are highlighted with a yellow dashed line.

3.2 Tape boundary

Local topology changes in terms of elevation were determined for top and bottom surfaces, as shown in Figure 3a-b. The surface variability shows an overall tendency to align in the fibre direction, with local surface misalignments from the longitudinal direction. The comparison

 ©2022 1st Author et al. https://doi.org/ 10.5075/978-X-XXX-XXXXX-X published under CC BY-NC 4.0 license

between the range of the surface elevation and the logarithm of differential tortuosity at the tape edge is reported in Figure 3c for both top and bottom tape surfaces. The results suggest a positive correlation between the standard deviation of elevation and the logarithm of differential tortuosity.

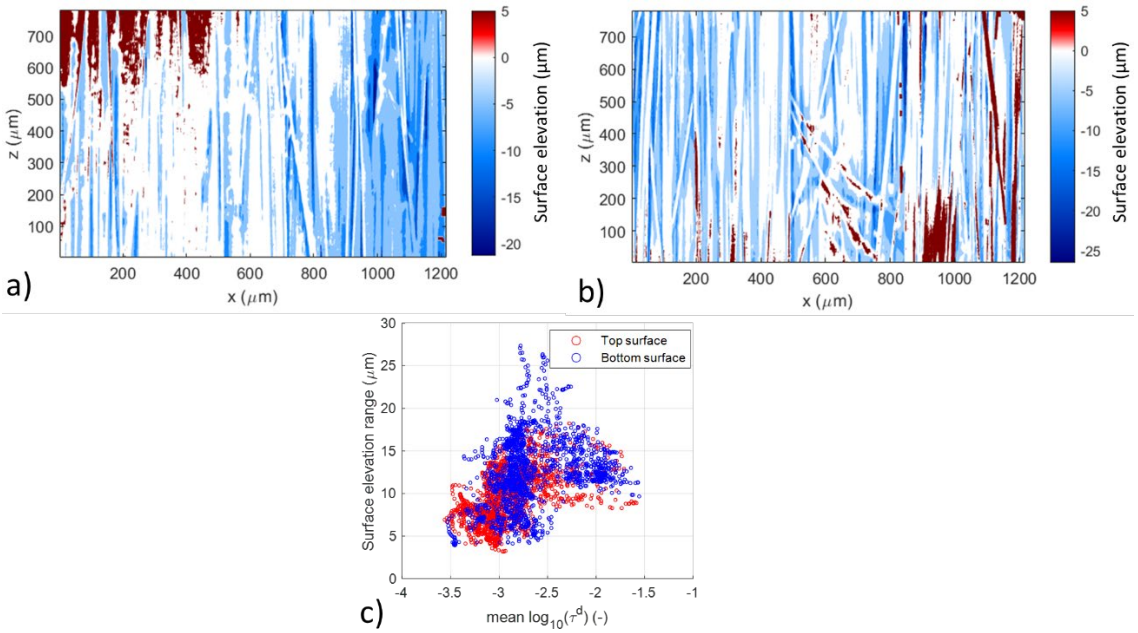

Figure 3. Surface elevation maps for a) top and b) bottom tape boundary; c) comparison of the surface elevation range calculated along the tape width and the correspondent values of the logarithm of differential tortuosity.

Surface variability effects are relevant to the understanding of the processability of unidirectional tapes [8]. Relating 3D surface variability and the underlying fibre architecture enables the extraction of surface fibre architecture information from the surface topology, potentially allowing the extraction of surface features during in-line monitoring. Approaches based on local fibre misalignment have been applied in the literature to estimate fibre alignment in composites from 2D micrographs [15], however 3D analysis of surface topology in relationship to underlying measured fibre tortuosity at the surface has not been reported for the study of unidirectional tapes to the authors' knowledge. The differential tortuosity map in Figure 2 shows corridors of higher tortuosity, which are both located along the bottom surface and running from the bottom-left to the top-right of the cross-section. Similar locations of surface elevation misalignment from the longitudinal direction can be located in Figure 3b. By comparing the surface elevation range to the tortuosity of the fibre architecture close to the boundary, it was possible to observe a positive correlation between the two, as shown in Figure 3c. The extent of the correlation between tape surface variability and fibre microstructure is expected to depend on the presence of resin-rich regions at the tape surface, which is minimal in this tape, as observed in Figure 1a.

3.3 Voids

The morphology and spatial distribution of voids was quantified via connected region analysis on the internal voids identified as in Section 2.2.1. Figure 4a shows a 3D representation of the distribution of the voids. The distribution of the voids aspect ratio between the longitudinal

 ©2022 1st Author et al. https://doi.org/ 10.5075/978-X-XXX-XXXXX-X published under CC BY-NC 4.0 license

dimension and the major cross-sectional dimension has been reported in Figure 4b, showing a tendency to void elongation in the longitudinal direction (values greater than 1). The void size distribution is shown in Figure 4c and spans over six orders of magnitude. The voids appear to be interfacial at a qualitative observation, being located at the fibre-matrix interface.

Since the voids tend to align along the fibre direction, their 2D accumulation for each location in the cross-section was considered, as reported in Figure 5a. The voids do not appear to be homogeneously distributed, but they seem to cluster in discrete regions. While low accumulation lengths were neglected, the cross-sectional void distribution for accumulation lengths greater than 100 µm was related to the logarithm of differential tortuosity. The mean logarithm of differential tortuosity was considered as a threshold for comparison. The regions where the logarithm of differential tortuosity is greater than its mean value are highlighted in yellow in Figure 5b. The histogram of Figure 5c reports the probability of void accumulation above and below the mean value of differential tortuosity and shows a greater probability of high void accumulation for high tortuosity values.

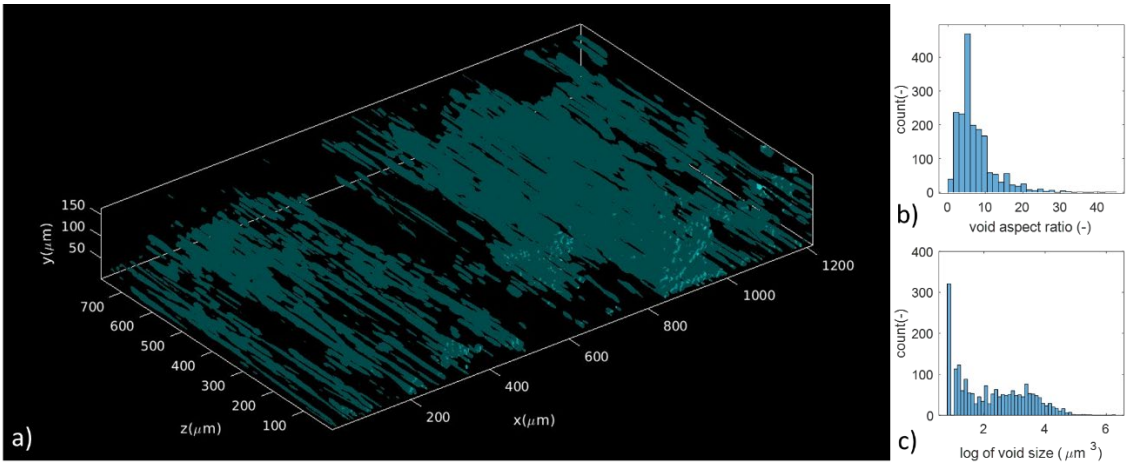

Figure 4. a) 3D representation of the internal void distribution in the scan volume. Statistics for the detected voids b) histogram of the aspect ratio of voids c) histogram of the distribution of the size of voids.

The sample considered shows interfacial voids between fibres and resin [16] elongated in the fibre length direction, as shown in Figure 4b, which is commonly observed in literature for UD composites [5,17]. Their presence might be attributed to incomplete impregnation. The comparison of the cross-sectional variability of voids and tortuosity of Figure 5c suggests that regions with high tortuosity have a higher probability of increased void formation. This might be related to hindering of the resin flow during impregnation. Conversely, regions with lower tortuosity, where fibre paths deviate less from the nominal alignment, show lower probability of voids presence.

4. Conclusion

A unidirectional composite tape was analysed accounting for both fibre-based descriptors, and matrix-based characteristics. The higher presence of defects in the development-grade material used compared to commercial grade tapes provides an opportunity to investigate links between tape boundary variability and void distribution to fibre-based descriptors such as differential tortuosity. The approach outlined in this work was able to describe the 3D microstructure at

 ©2022 1st Author et al. https://doi.org/ 10.5075/978-X-XXX-XXXXX-X published under CC BY-NC 4.0 license

both fibre and matrix level in unidirectional composite tapes. Future work should further investigate these emerging relationships in their broader application to unidirectional tapes and composites.

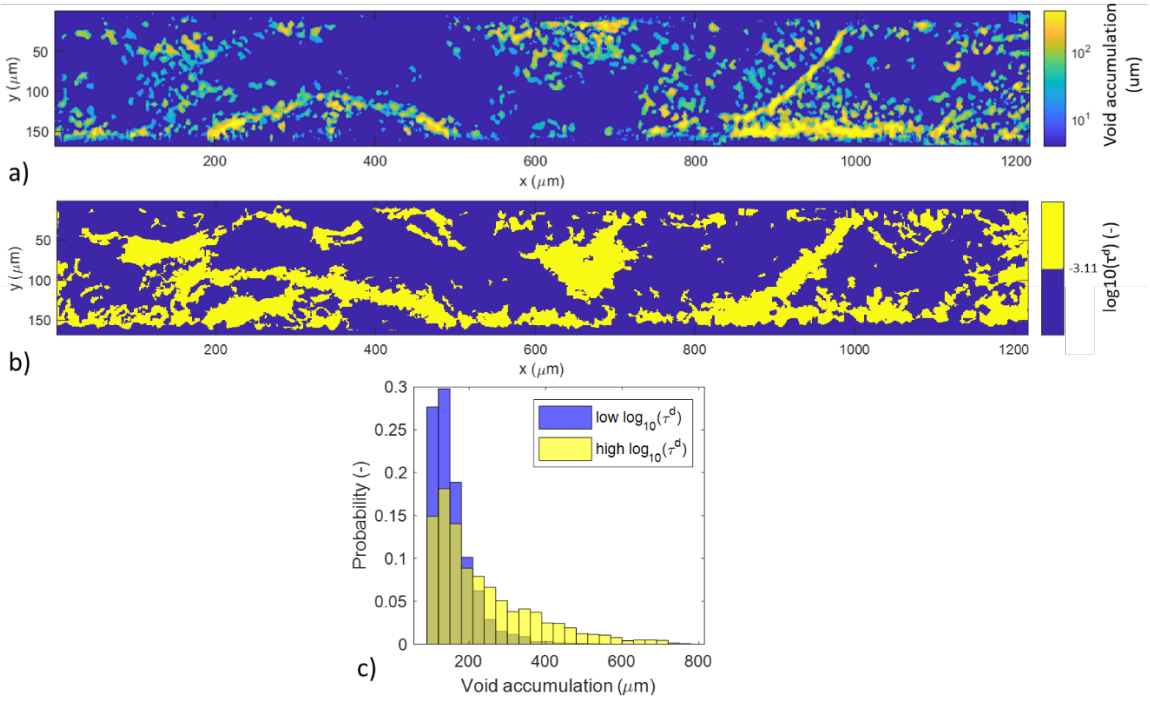

Figure 5. a) 2D histogram of the voids distribution in the cross-section b) map which highlights in yellow the regions where the logarithm of differential tortuosity is greater than its mean value c) histogram of the void accumulation for high value of the logarithm of differential tortuosity (above the mean value) and for low values (below the mean value).

Acknowledgements

The authors would like to acknowledge Naturalis Biodiversity Centre (Leiden, Netherlands) for conducting the X-ray computed tomography measurements, and Onur Yüksel (Aerospace Manufacturing Technologies group, Delft University of Technology, Delft, Netherlands) for the valuable discussions.

5. References

1. Gommer F, Wedgwood KCA, Brown LP. Composites : Part A Stochastic reconstruction of filament paths in fibre bundles based on two-dimensional input data. Compos PART A. 2015;76:262–71.
2. Gommer F, Endruweit A, Long AC. Quantification of micro-scale variability in fibre bundles. Compos Part A Appl Sci Manuf. 2016;87(January):131–7.
3. Emerson MJ, Wang Y, Withers PJ, Conradsen K, Dahl AB, Dahl VA. Quantifying fibre reorientation during axial compression of a composite through time-lapse X-ray imaging and individual fibre tracking. Compos Sci Technol. 2018;168(August):47–54.
4. Mehdikhani M, Breite C, Swolfs Y, Wevers M, Lomov S V., Gorbatikh L. Combining digital image correlation with X-ray computed tomography for characterization of fiber orientation in unidirectional composites. Compos Part A Appl Sci Manuf.

 ©2022 1st Author et al. https://doi.org/ 10.5075/978-X-XXX-XXXXX-X published under CC BY-NC 4.0 license

2021;142(September 2020):106234.
5. Mehdikhani M, Gorbatikh L, Verpoest I, Lomov S V. Voids in fiber-reinforced polymer composites: A review on their formation, characteristics, and effects on mechanical performance. J Compos Mater. 2019;53(12):1579–669.
6. Krämer ETM, Grouve WJB, Koussios S, Warnet LL, Akkerman R. Real-time observation of waviness formation during C/PEEK consolidation. Compos Part A Appl Sci Manuf [Internet]. 2020;133(January):105872.
7. Gomarasca S, Peeters DMJ, Atli-Veltin B, Dransfeld C. Characterising microstructural organisation in unidirectional composites. Compos Sci Technol. 2021;215(July):109030.
8. Çelik O, Peeters D, Dransfeld C, Teuwen J. Intimate contact development during laser assisted fiber placement: Microstructure and effect of process parameters. Compos Part A Appl Sci Manuf. 2020;134(February):105888.
9. Hapke J, Gehrig F, Huber N, Schulte K, Lilleodden ET. Compressive failure of UD-CFRP containing void defects: In situ SEM microanalysis. Compos Sci Technol. 2011;71(9):1242–9.
10. Katuin N, Peeters DMJ, Dransfeld CA. Method for the microstructural characterisation of unidirectional composite tapes. J Compos Sci. 2021;5(10).
11. Çelik O, Peeters D, Dransfeld C, Teuwen J. Intimate contact development during laser assisted fiber placement: Microstructure and effect of process parameters. Compos Part A Appl Sci Manuf. 2020;134(December 2019):105888.
12. Schindelin J, Arganda-Carreras I, Frise E, Kaynig V, Longair M, Pietzsch T, Preibisch S, Rueden C, Saalfeld S, Schmid B, Tinevez JY, White DJ, Hartenstein V, Eliceiri K, Tomancak P, Cardona A. Fiji: An open-source platform for biological-image analysis. Nat Methods. 2012;9(7):676–82.
13. Arganda-Carreras I, Kaynig V, Rueden C, Eliceiri KW, Schindelin J, Cardona A, Seung HS. Trainable Weka Segmentation: A machine learning tool for microscopy pixel classification. Bioinformatics. 2017;33(15):2424–6.
14. Tinevez JY, Perry N, Schindelin J, Hoopes GM, Reynolds GD, Laplantine E, Bednarek SY, Shorte SL, Eliceiri KW. TrackMate: An open and extensible platform for single-particle tracking. Methods. 2017;115:80–90.
15. Raimondi L, Brugo TM, Zucchelli A. Fiber misalignment analysis in PCM-UD composite materials by Full Field Nodal Method. Compos Part C Open Access. 2021;5(May):100151.
16. Çelik M, Noble T, Jorge F, Jian R, Br MÓ, Robert C. Influence of Line Processing Parameters on Properties of Carbon Fibre Epoxy Towpreg. J. Compos. Sci 2022;*6*(3):75
17. Comer AJ, Ray D, Obande WO, Jones D, Lyons J, Rosca I, Higgins RMO, Mccarthy MA. Composites : Part A Mechanical characterisation of carbon fibre – PEEK manufactured by laser-assisted automated-tape-placement and autoclave. Compos PART A. 2015;69:10–20.

 ©2022 1st Author et al. https://doi.org/ 10.5075/978-X-XXX-XXXXX-X published under CC BY-NC 4.0 license